Proceedings of the 17th World Congress
The International Federation of Automatic Control
Seoul, Korea, July 6-11, 2008

Adaptive Bolus Chasing Computed Tomography Angiography

Er-Wei Bai, Ph.D.,Zhijun Cai, Ph.D., * **Ge Wang, Ph.D.** **

* *Electrical and Computer Engineering, The University of Iowa, Iowa City, IA 52242, USA (e-mail: er-wei-bai, zhijun-cai@uiowa.edu).*
** *VT-WFU School of Biomedical Eng. & Sci., Virginia Polytechnic Institute & State University, Blacksburg, VA 24061, USA (e-mail: wangg@vt.edu)*

Abstract: Synchronization of the contrast bolus peak and CT imaging aperture is a crucial issue for CTA. It effects the CTA imaging quality and the necessary amount of contrast dose. In this paper, we propose an optimal adaptive bolus chasing controller. The controller estimates and predicts the unknown two dimensional bolus density on line and then determines the optimal control actions. Tracking errors are mathematically quantified in terms of estimation errors. Simulation results on the actual patient data exhibit its superior performance to the current constant-speed method. Also, the preliminary experiments demonstrate the clinical feasibility.

Keywords: adaptive control; optimal control; control algorithm; medical systems; Computed Tomography (CT); CT Angiography (CTA).

1. INTRODUCTION

Today, Computed Tomography Angiography (CTA) has become an important investigative tool for vascular disease with the advent of multi-row CT Fuchs et al. [2003], Jakobs et al. [2004]. To better define the vasculature from its surrounding soft tissue, a dose of contrast medium (a contrast bolus) is injected into a vein through an IV (intravenous) tube. During the scanning, the contrast medium propagates in the artery, and meanwhile the patient is fed into the CT gantry by translating the CT table. It is highly desirable to scan the blood vessels with the highest density contrast medium inside. Therefore, synchronizing the contrast bolus peak and CT imaging aperture is crucial to the CTA results. Unfortunately, the contrast bolus dynamics are highly nonlinear, complicated, and influenced by many factors, e.g., patient weight, vasculature diseases, and injection patterns. In current practice, the CT table moves at a preset constant speed, and is very likely to miss the bolus peak. To compensate for this problem, a large amount of contrast medium is needed, which is harmful to the patient's kidney. Bae [2003], Cademartiri et al. [2002].

The current existing bolus chasing techniques only mean to chase the bolus arrival, which determines CT table starting time. The techniques can be categorized into two classes: ROI (Region Of Interest) threshold triggering Schweiger et al. [1998], Cademartiri et al. [2002] and the timing bolus Hittmair and Fleischmann [2001], Bae [2005]. The former technique sets a threshold (bolus density represented by HU) at a specific position, e.g., aorta, which is being monitored after the injection. When the observed density reaches the threshold, the CT table is automatically started. However, it is very difficult for the operators to choose the correct threshold Paulson et al. [1998]. If it is set too low, the CT table will be started too early. If it is set too high, the CT table might not be started at all. The other technique calls for an injection of a small amount contrast medium prior to the main injection used for diagnosis. The time between the injection to the vein and peak density appearance in the ROI is taken as the delay time (may be added by several seconds) to start the CT table for the main injection. Obviously, it is assumed that the timing bolus and actual bolus have the same peak arrival time, which may not be true in most cases Cademartiri et al. [2002]. Furthermore, it requires an additional injection and test time, which increases the contrast dose and the diagnosis time.

Even when the right bolus arrival time to the designated ROI is obtained, there is no guarantee of the synchronization of the bolus peak and imaging aperture during the CT exam due to the complicated bolus dynamics. Consequently, many researchers try to make the resulting bolus profile more conducive to the preset constant-speed method by means of varying the injection rate and duration, called bolus geometry optimization method Schweiger et al. [1998], Bae et al. [1998], Backer et al. [2003], Fleischmann and Hittmair [1999], Kopka et al. [2004]. They expect that if a bolus keeps its maximum density for a longer time at a position, then the synchronization is easier to be obtained. As a result, many injection protocols were reported, such as multiple-injection method Rossi et al. [1982] and the inverse method Fleischmann and Hittmair [1999]. However, this method requires a priori knowledge of the patients vascular system to achieve the desirable results, which cannot be known before a preliminary injection. To that end, it may end up with a larger amount of contrast dose, which is not good for patients.

⋆ This work was supported by NIH.

The effective and robust way to chase the bolus peak is the adaptive method, which predicts the bolus peak using the online CT images and varies the CT table speed accordingly. This concepts has been studied in other imaging modalities, such as Digital Subtraction Angiography (DSA) Wu and Qian [1998] and Magnetic Resonance Angiography (MRA) Wang et al. [1998], Ho et al. [1999]. Preferable results have been reported in these studies. However, there are few studies on bolus chasing CTA due to the small field of view (z direction) for CTA and the complicated CT image reconstruction algorithm with varying pitch. Recently, we have developed the CT image reconstruction algorithms for varying pitch Yu et al. [2005] and extensively studied the bolus characteristics Cai et al. [2006], Bennett [2003].

2. CONTRAST BOLUS CHARACTERISTIC AND PROBLEM STATEMENT

2.1 Contrast bolus characteristics

The contrast bolus dynamics are extremely complicated and many researchers have tried different methods to describe bolus dynamics. In Bae et al. [1998], Wang et al. [2000], physiologic models of contrast enhancement are developed, which incorporate injection methods, physiologic data and contrast pharmaceutics. However, the proposed models are too complicated for practical use and they are sensitive to many unknown parameters which are impossible to estimate on line. On the other hand, the bolus density is simply a function of time and distance and people are interested in the bolus time-density (attenuation) curves at some ROIs. For example, Blomley and Dawson [1997] used a gamma variate function to fit the bolus time-attenuation curve in the aorta. However, the best fit model so far is the lagged normal density model proposed by Bassingthwaighte et al. [1966]. We extend it into two dimension

$$B(t,z) = C(z)\frac{1}{\sigma(z)\sqrt{2\pi}}e^{-\frac{(t-t_c)^2}{2\sigma(z)^2}} * \frac{1}{\tau(z)}e^{-\frac{t}{\tau(z)}}, \qquad (1)$$

where $*$ denotes the convolution operation. This is actually a linear system of infinite order. The coefficient $C(z)$ relies on the injection (input) pattern. At a fixed location z, C, σ, t_c and τ are constants. We test this model for more than hundred data sets, which are MRA timing-bolus data of the aorta and were collected from University of Iowa Hospital and Clinic (UIHC) and Northwestern university (NU). It is shown that (1) has the ability to fit the actual model very well Cai et al. [2006]. Figure 1 is a typical bolus profile in the aorta, where (a) denotes time-distance-density profile, (b) is the bolus contour, (c) is the bolus temporal curve at a position, and (d) is the bolus spatial curve at a time. Here, the bolus density is represented by the signal intensity, which is proportional to the bolus density.

It is very interesting to observe that both the actual bolus time-density curves and the model reveal intrinsic properties of the contrast bolus dynamics. As far as the control design is concerned, the most important property is: At any given position z, the bolus density $B(t,z)$ is monotonically (not necessarily strictly) increasing in time t before it reaches the maximum and is monotonically

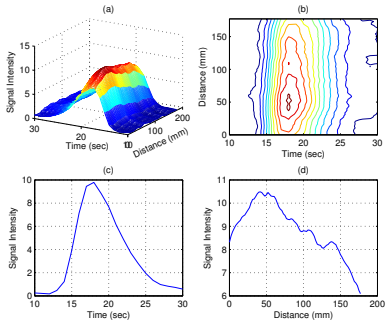

Fig. 1. Actual bolus time-distance-density profile in the aorta,(a)time-distance-density profile, (b) bolus contour, (c) bolus time-density curve at a position, and (d) bolus distance-density curve at certain time.

(not necessarily strictly) decreasing after that. Since this property is frequently used in the paper, we define such a function as a class $\mathcal{A}$ function.

Definition 1. A differentiable function $f(t)$ is said to belong to the class $\mathcal{A}$ if

(1) There exists a maximum point t^* such that $t^* = \arg\max_t f(t)$,
(2) $f(t)$ is monotonically (not necessarily strictly) increasing for $t \in (-\infty, t^*]$ and monotonically (not necessarily strictly) decreasing for $t \in [t^*, \infty)$.

2.2 Problem Statement

The overall goal of the adaptive bolus chasing CTA is to design an adaptive controller to synchronize the bolus peak and imaging aperture. It is achieved by instantaneously processing the bolus CT images, dynamically predicting the bolus peak position, and adaptively moving the CT table in the opposite direction to follow the bolus peak. Let the bolus density function be given by $B(t,z)$ where t represents time ($t=0$ corresponds to the injection instant) and z represents distance ($z=0$ corresponds to the initial monitored position). Also let the scan range be divided into N segments, that is, $z_k = k\frac{z_e}{N}$, $k = 0 \ldots N$, where z_e is the scan distance. The control objective is to find a time sequence, $\{t^*(z_k)\}_{k=1}^N$, such that

$$J_c = \sum_{i=1}^{N} B(t(z_i), z_i) \qquad (2)$$

is maximized. The motivation behind (2) is to maximize the average density over the whole scan length, which results in overall better quality CT images for every position of the blood vessel.

3. CONTROLLER DESIGN

3.1 Control with no constraints

In case that $B(t,z)$ is known and there is no constraints on the CT table velocity, the solution of problem (2) is given by

$$t^*(z_k) = \arg\max_{t(z_k)} B(t(z_k), z_k) \quad k = 1, \ldots, N. \qquad (3)$$

As discussed before, however, the exact profile $B(t,z)$ is not known throughout the scanning. Determination of the optimal $t^*(z_k)$'s has to rely on a sequence of local approximations $\{\widehat{B}_k(t,z_{k+1})\}_{k=0}^{N-1}$ and

$$\bar{t}(z_k) = \arg\max_{t(z_k)} \widehat{B}_{k-1}(t(z_k), z_k), \quad k = 1, \ldots, N. \tag{4}$$

There are two questions. The first is how to find such approximations $\{\widehat{B}_k(t,z_{k+1})\}_{k=0}^{N-1}$ which is the topic of estimation. The second question is how small the error $t^*(z_k) - \bar{t}(z_k)$ is and more importantly, how close $B(t^*(z_k), z_k)$ and $B(\bar{t}(z_k), z_k)$ is that is what we are really after. Intuitively, if $\widehat{B}_{k-1}(t,z_k)$ approximates $B(t,z_k)$ well in the vicinity of $t^*(z_k)$, we expect a small error.

3.2 Control with constraints

In equations (3) and (4), it is apparent that $\bar{t}(z_k)$ and $t^*(z_k)$ need not be strictly increasing sequences which is problematic for real time implementation. Also, the table's speed is bounded by mechanical factors and patient comfort, i.e., the table speed should be limited by lower and upper bounds

$$0 < \frac{z_e/N}{\Delta_b} \le \frac{dz}{dt} \le \frac{z_e/N}{\Delta_s} < \infty$$

for some Δ_b and $\Delta_s > 0$, where z_e/N is the length of each section. Or equivalently,

$$0 < \frac{\Delta_s}{z_e/N} \le \frac{dt}{dz} \le \frac{\Delta_b}{z_e/N} < \infty.$$

This translates into the constraint

$$0 < \Delta_s \le\ t(z_{k+1}) - t(z_k) \le \Delta_b < \infty,\ k = 0, \ldots, N-1 \tag{5}$$

Therefore, the control laws have to be modified considering the above constraint. If $B(t,z)$ is known, the solution is now given by

$$t_k^* = \begin{cases} t_k^* = t_{k-1}^* + \Delta_s, & \text{if } t^*(z_k) \le t_{k-1}^* + \Delta_s \\ t_k^* = t_{k-1}^* + \Delta_b, & \text{if } t^*(z_k) \ge t_{k-1}^* + \Delta_b \\ t_k^* = t^*(z_k), & \text{otherwise.} \end{cases} \tag{6}$$

where $t^*(z_k) = \arg\max_t B(t,z_k)\ \ k = 1, \ldots, N$.

Similarly, if $B(t,z)$ is unavailable, the control based on its estimates $\widehat{B}_{k-1}(t,z_k)$'s is given by

$$\bar{t}_k = \begin{cases} \bar{t}_k = \bar{t}_{k-1} + \Delta_s, & \text{if } \bar{t}(z_k) \le \bar{t}_{k-1} + \Delta_s \\ \bar{t}_k = \bar{t}_{k-1} + \Delta_b, & \text{if } \bar{t}(z_k) \ge \bar{t}_{k-1} + \Delta_b \\ \bar{t}_k = \bar{t}(z_k), & \text{otherwise.} \end{cases} \tag{7}$$

where $\bar{t}(z_k) = \arg\max_t \widehat{B}_{k-1}(t,z_k),\ k = 1, \ldots, N$.

We now quantify the errors between $t_k^* - \bar{t}_k$ and $B(t_k^*, z_k) - B(\bar{t}_k, z_k)$.

Theorem 1. Let $B(t,z_k)$ and $\widehat{B}_{k-1}(t,z_k)$ belong to class $\mathcal{A}$ at each z and $\left|\frac{\partial B(t,z_k)}{\partial t}\right| \le \epsilon$, for $\forall\, t,k$. Suppose there exists a positive $\delta > 0$, and

$|B(t,z_k) - \widehat{B}_{k-1}(t,z_k)| \le \delta,\ \ t \in [t^*(z_k) - d_k, t^*(z_k) + d_k]$, where $d_k = \max\{|t^*(z_k) - t_1(z_k)|, |t^*(z_k) - t_2(z_k)|\}$ and $t_1(z_k) < t^*(z_k)$ $(t_2(z_k) > t^*(z_k))$ is the maximum (minimum) value such that $B(t_1(z_k), z_k) \le B(t^*(z_k), z_k) - 2\delta$ $(B(t_2(z_k), z_k) \le B(t^*(z_k), z_k) - 2\delta)$. Let $d = max_k\,\{d_k\}$ and assume that $\widehat{B}_{k-1}(t,z_k)$ is not constant in $t \in [t_1(z_k), t_2(z_k)]$. If t_k^* and $\bar{t}_k$ denote the sequences resulting from (6) and (7), respectively, then we have

$$|t_k^* - \bar{t}_k| \le d \text{ and } |B(t_k^*, z_k) - B(\bar{t}_k, z_k)| \le d \cdot \epsilon$$

for $k = 1, \ldots, N$, if $|t_0^* - \bar{t}_0| \le d$.

Proof: See Bai et al. [2008].

3.3 Online estimation of $B(t,z)$

Since $B(t,z)$ is unavailable, calculation of the control law relies on the estimates $\widehat{B}_{k-1}(t,z_k)$. As shown in the previous subsection, if the estimate $\widehat{B}_{k-1}(t,z_k)$ is close to the true but unknown $B(t,z)$ locally, the effect of approximation is negligible. However, $\widehat{B}_{k-1}(t,z_k)$ has to be estimated in real time solely based on observed local bolus information. On one hand, the approximation error depends on how rich the structure of the approximation $\widehat{B}_{k-1}(t,z_k)$ is that incorporates well the local bolus information into its representation. On the other hand, the structure should be simple enough so that it can be easily estimated on line. There is a trade off between approximation ability and estimation accuracy. A natural choice of $\widehat{B}_{k-1}(t,z_k)$ is a polynomial. The order of the polynomial balances the ability to approximate $B(t,z)$ and the estimation simplicity. We consider a second order polynomial,

$$\begin{aligned} B(t,z) &\approx B(t_k,z_k) + \nabla_t B|_{(t_k,z_k)}(t-t_k) + \nabla_z B|_{(t_k,z_k)}(z-z_k) \\ &\quad + \frac{1}{2}\begin{pmatrix} t-t_k \\ z-z_k \end{pmatrix}^T \nabla^2 B|_{(t_k,z_k)} \begin{pmatrix} t-t_k \\ z-z_k \end{pmatrix} \\ &= a_0 + a_1 t + a_2 z + a_3 t^2 + a_4 zt + a_5 z^2, \end{aligned} \tag{8}$$

for some a_0, a_1, a_2, a_3, a_4 and a_5, which will be estimated on line. Another important factor is the selection of approximation data. Obviously, the smaller the region, the better a second order polynomial can approximate $B(t,z)$. On the other hand, we would like the approximation function to give us some information about the bolus away from the observation points. This implies that the approximation region cannot be too small. In addition, realistic CT specifications have to be considered.

- CT is assumed to have multiple rows of detectors.
- CT gantry rotation speed is set to $\Delta T = 1/3$ second per rotation, a standard in modern CT.
- The maximum patient table speed in a modern CT is about $10 cm/sec$ Fuchs et al. [2003], which sets the lower bound Δ_s in the constraint.
- The minimum speed is set to 0 cm/sec which ensures that the patient table does not go back, a standard practice. This sets the upper bound Δ_b.

With these constraints, data points of $B(t,z)$ at $\bar{t}_k, \bar{t}_{k-1}$, $\bar{t}_{k-2}$ and $z = z_k, z_k \pm \delta z$ are collected for each rotation of the gantry. These data are used to identify the a_i's in the second order approximation in the least squares sense

$$\begin{aligned} \hat{a}_i = \arg\min_{a_i} \sum_{z=z_k, z_k \pm \delta z,\ t=\bar{t}_k, \bar{t}_{k-1}, \bar{t}_{k-2}}^{3} \big\{ & B(t,z) \\ & - (a_0 + a_1 t + a_2 z + a_3 t^2 + a_4 zt + a_5 z^2) \big\}^2. \end{aligned} \tag{9}$$

Further, the next $\bar{t}_{k+1}$ is determined from (7) with $\widehat{B}_k(t, z_{k+1}) = \hat{a}_0 + \hat{a}_1 t + \hat{a}_2 z_{k+1} + \hat{a}_3 t^2 + \hat{a}_4 z_{k+1} t + \hat{a}_5 z_{k+1}^2$.

4. SIMULATION RESULTS ON THE PATIENT DATA

The proposed control scheme has been tested on the actual clinical data collected from UIHC and NU. In the simulations, the upper and lower bounds Δ_b, Δ_s and ΔT are set as mentioned in section 3.3 and z_e/N is set to be 5mm. To show its superiority, the proposed adaptive control is compared to the performance of the existing technology, a constant speed control of the patient table, i.e., $t_k = cz_k + t_0$ for some constant c. A common practice in clinic is to set c so that the table speed is at 3 cm/sec Fleischmann et al. [2006].

Two comparisons are made. The first is the achieved bolus density. To this end, we define

$$I_a = \frac{\sum B(t_k^*, z_k)}{\sum B(t^*(z_k), z_k)}, \quad I_c = \frac{\sum B(cz_k + t_0, z_k)}{\sum B(t^*(z_k), z_k)}$$

where c is chosen so the constant speed control is at 3 cm/sec. $\sum B(t^*(z_k), z_k)$ is the maximum achievable bolus density. $\sum B(t_k^*, z_k)$ and $\sum B(cz_k + t_0, z_k)$ are the actually achieved bolus densities for the adaptive control and the constant speed control respectively. Typical tracking results for both adaptive and constant-speed method are shown in Figure 4, where the top plots show the bolus contour (solid thin curve: the inner the curve, the higher the density), the bolus peak trajectory (dashed), adaptive bolus chasing trajectory (thick solid) and constant-speed trajectory (dash dot); and the bottom plots show the maximum achievable bolus density at each position z_k (dashed), the achieved bolus density by the adaptive control (solid) and the achieved bolus density by the constant-speed method (dash dot). Table 1 summarizes the performance index for ten patients. Clearly, in all cases the proposed adaptive control outperforms the current constant-speed method significantly.

Table 1. Performance index of adaptive method and constant-speed method

UIHC patient	I_a	I_c	NU patient	I_a	I_c
patient 1	0.98	0.90	patient 1	0.99	0.93
patient 2	0.95	0.78	patient 2	0.98	0.85
patient 3	0.93	0.74	patient 3	0.97	0.81
patient 4	0.95	0.83	patient 4	0.99	0.90
patient 5	0.93	0.84	patient 5	0.98	0.58

The second performance to be compared is the robustness with respect to the the triggering threshold variation. Recall that the table movement is initially triggered by a preset threshold Cademartiri et al. [2002]. As for the constant-speed method, if the threshold is set too low or too high, the CT performance deteriorates. While the adaptive method has the ability to determine the optimal action, therefore its performance does not rely on the threshold settings. Figure 4 shows the threshold variation results of adaptive control and constant-speed method on a patient data set. Obviously, The best performance of the constant-speed method is not obtained at the highest threshold nor at the lower threshold in the plot. This poses a difficult problem for the constant-speed method. On the other hand, the adaptive-optimal control performs uniformly well independent of various threshold settings.

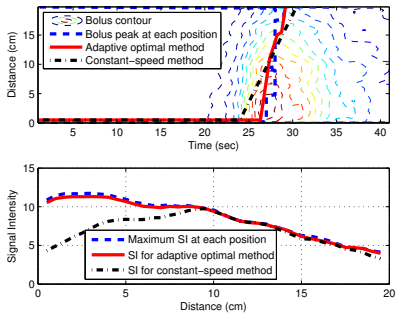

Fig. 2. Typical tracking result on a patient data collected from UIHC.

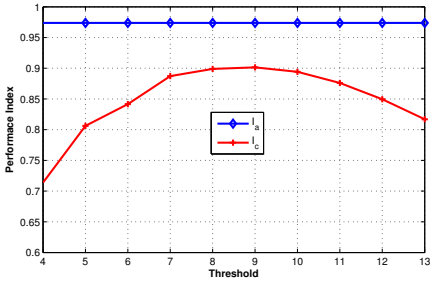

Fig. 3. Performance on NU Patient 3 of adaptive-optimal method (solid diamond) and constant-speed method with different threshold (dashed cross).

5. EXPERIMENT ON THE REAL CT SCANNER

Recently, we have demonstrated the adaptive bolus chasing CTA concept on a real CT scanner.

5.1 Experimental setup

CT scanner The CT scanner is a Siemens Somatom Volume Zoom four-slice CT scanner with software version A40A. Due to the proprietary issue, there are two delays of the closed-loop control system: an image display delay and a control delay. The image display delay is caused by the image reconstruction and display on the monitor, while the control delay is caused by CANbus communication and table movement execution. Both delays pose a very serious challenge for controller design. It is important to comment that the combined control delay is caused by the CANbus. If the full proprietary control commands are available to us, the control delay problem is nonexistent. We are currently working with Siemens to try to have those full proprietary control commands in the near future. All the results reported in this paper are under the control delay constraint.

Frame grabber Although we have the CT reconstruction algorithm for varying pitch, we are not able to reconstruct the CT images due to the unavailability of the proprietary raw data. Therefore, the only possible feedback of the bolus density is the real time CT image on the monitor. To that end, we split the CT VGA signal, feed it to the controller, and capture it using a frame grabber.

Blood flow system A programmable MasterFlex pump system connected with a plastic tube filled with water will be used to simulated the heart outflow and the

vasculature. During the experiment, we adjust the pump speed to achieve the desirable bolus dynamics. Roughly speaking, the bolus speed is proportional to the pump flow rate, though in reality it is not exactly proportional because of the irregularity of the tube and discontinuity of the flow.

Contrast bolus replacement Due to the delay issues, we have to scale down the actual bolus velocity. However the liquid contrast bolus dilutes in the water in a short time, which is not feasible to chase. To that end, we replace it with a solid bolus. To mimic the actual bolus characteristics, the solid bolus is tapered at both ends, and its cross-sectional area is used as the average density at that position. Further in the experiment, the cross-sectional area is represented by pixel number in that area.

5.2 Experimental results

To compare the performance of the adaptive chasing method and the current constant-speed method, we applied both methods on the same bolus flow pattern. One of the tracking results on the real CT are shown in Figure 5.2 and 5.2 for adaptive chasing method and constant-speed method, respectively. In Figure 5.2 and 5.2, the top plots give the CT table movement trajectory, while the bottom plots show the observed density (represented by the pixel number) with the corresponding table movement. In the experiment, the bolus is managed to be stopped during $35sec$ and $60sec$, which mimics the case when it meets an aneurysm. Two different constant table speeds: $4mm/s$ and $3.5mm/s$ are used for constant-speed method. As we expect, the adaptive chasing method tracks the bolus very well throughout the experiment (see bottom plot of Figure 5.2), while the results of the constant-speed are unsatisfactory. The CT table that moves at a constant speed of $4mm/s$ only catches the bolus at the very beginning, and loses the bolus after 40 seconds, while the table moving at $3.5mm/s$ catches the bolus thrice and only scans the bolus peak for a few seconds. To make a quantitative comparison, we compute the average scanned densities over the scanning duration for both the adaptive chasing method and the constant-speed methods, along with their percentages of the maximum density (2500) as shown in Table 2. It is clear that the adaptive chasing method follows close to the bolus peak (88.5%), while the constant-speed methods have poor performances, 10.4% and 30.9% for $4mm/s$ and $3.5mm/s$, respectively.

Table 2. The average scanned density of the adaptive chasing method and the constant-speed methods.

Method	Adaptive chasing	$4mm/s$ constant	$3.5mm/s$ constant
Average density	2212	260	772
Percentage of the maximum	88.5 %	10.4 %	30.9 %

Based on the normalized scanned bolus density, we reconstruct the 3D plastic tubes, which represent blood vessels, and are shown in Figure 5.2, where the left, middle and right "blood vessels" are reconstructed using the data for the adaptive tracking method, the 4mm/s constant CT table method, and the 3.5 mm/s method, respectively. Obviously, the 3D "blood vessel" based on the adaptive

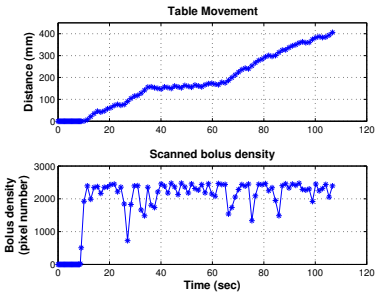

Fig. 4. The experimental results for varying pump speed. Top plot: the table position with respect to time; Bottom plot: The scanned bolus density over time.

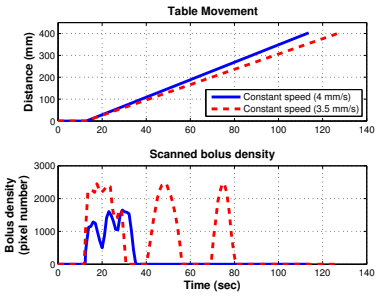

Fig. 5. The experimental results for two different constant table speeds (solid line is for 4mm/s and dashed line is for 3.5mm/s). Top plot: the table position with respect to time; Bottom plot: The scanned bolus density over time.

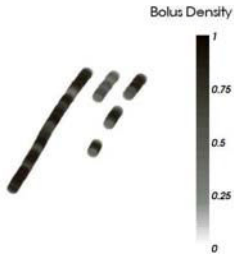

Fig. 6. The reconstructed 3D blood vessels of adaptive tracking method (left), 4mm/sec constant speed method (middle), and 3.5mm/sec constant speed method (right).

tracking method is fully reconstructed, while the constant CT table speed methods do not show the whole "blood vessel". The reason for this is that the adaptive chasing method scanned the "blood vessel" from the beginning to the end with the peak of the bolus of contrast, while the constant speed methods did not.

6. CONCLUSION

In this paper, we proposed an adaptive control algorithm for bolus chasing CTA, which incorporates the CT image reconstruction, online biomedical image analysis and adaptive control techniques. Both online simulations on clinical data sets and experiments on real CT scanner show that the proposed algorithm has a great potential in tracking the bolus with the highest density. Comparisons

against the constant-speed methods convinces us that the proposed algorithm is promising. The future work will be focused on clinical trials.

REFERENCES

K.T. Bae, J.P. Heiken and J.A. Brink. Aortic and hepatic contrast medium enhancement at CT. Part I. Prediction with a computer model. *Radiology*, 207, pages 647–655, 1998.

K.T. Bae. Technical aspects of contrast delivery in advanced CT. *Supplement to Applied Radiology*, 32, pages 12–19, 2003.

K.T. Bae. test-bolus versus bolus-tracking techniques for CT angiographic timing. *Radiology*, 236(1), pages 369–370, author reply 370., 2005.

C.R. Backer, C. Hong, A. Knez, A. Leber, R. Bruening, U.J. Schoepf and M.F. Reiser. Optimal contrast application for cardiac 4-detector-row CT. *Investigative Radiology*, 38(11), pages 690–694, 2003.

E.W. Bai, Z. Cai, R. McCabe and G. Wang. (2008). An Adaptive Optimal Control Design for a Bolus Chasing Computed Tomography Angiography. *IEEE Transactions on Control Systems Technology*, Vol. 16, No. 1, pp 60-69, 2008.

J.R. Bennett, E.W. Bai, J.I. Halloran and G. Wang A preliminary study on adaptive field-of-view tracking in peripheral digital subtraction angiography. *Journal of X-Ray Science and Technology*, 14(1), pages 27–38, 2006.

J.B. Bassingthwaighte, F.H. Ackerman and E.H. Wood. Applications of the lagged normal density curve as a model for arterial dilution curves. *Circulation Research*, 18, pages 398–415, 1966.

M.J. Blomley and P. Dawson Bolus dynamics: Theoretical and experimental aspects. *The British Journal of Radiology*, 70, pages 351–359, 1997.

F. Cademartiri, A. van der Lugt, G. Luccichenti, P. Pavone and G.P. Krestin. Parameters Affecting Bolus Geometry in CTA: A Review. *Journal of Computer Assisted Tomography*, 26(4), pages 598–607, 2002.

Z. Cai, A. Stolpen, M. Sharafuddin, R. McCabe, H. Bai, T. Potts, M. Vannier, D. Li, X. Bi, J.R. Bennett, J. Golzarian, S. Sun, G. Wang and E.W. Bai. Bolus characteristics based on MRA data. *BioMedical Engineering OnLine*, 17Oct2006.

D. Fleischmann and K. Hittmair. Mathematical analysis of arterial enhancement and optimization of bolus geometry for ct angiography using the discrete Fourier transform. *Journal of Computer Assisted Tomography*, 23(3), pages 474–484, 1999.

D. Fleischmann, R.L. Hallett and G.D. Rubin. CT angiography of peripheral arterial disease. *Journal of Vascular and Interventional Radiology*,17(1), pages 3–26, 2006.

T.O.J. Fuchs, M. Kachelrieb and W.A. Kalender. Fast Volume Scanning Approaches by X-Ray-Computed Tomography. *Proceedings of the IEEE*,Vol. 91, No. 10, pages 1492–1502, 2003.

K. Hittmair and D. Fleischmann. Accuracy of Predicting and Controlling Time-Dependent Aortic Enhancement from a Test Bolus Injection. *Journal of Computer Assisted Tomography*,25(2), pages 287–294, 2001.

V.B. Ho, P.L. Choyke, T.F.K. Foo, M.N. Hood, D.L. Miller, J.M. Czum and A.M. Aisen. Automated Bolus Chase Peripheral MR Angiography: Initial Practical Experiences and Future Directions of This Work-In-Progress. *Journal of Magnetic Resonance Imaging*,10(3), pages 376–388, 1999.

T. Jakobs, B. Wintersperger and C. Becker MDCT-Imaging of Peripheral Arterial Disease. *Seminars in Ultrasound, CT, and MRI*,25(2), pages 145–155, 2004.

L. Kopka, J. Rodenwaldt, U. Fischer, D.W. Mueller, J.W. Oestmann and E. Grabbe. Dual-phase helical CT of the liver: Effects of bolus tracking and different volumes of contrast material. *Radiology*,201, pages 321–326, 2004.

D.G. Kruger, S.J. Riederer, J.A. Polzin, A.J. Madhuranthakam, H.H. Hu and J.F. Glockner. Dual-Velocity Continuously Moving Table Acquisition for Contrast-Enhanced Peripheral Magnetic resonance Angiography. *Magnetic Resonance in Medicine*,53(1), pages 110–117, 2005.

E.K. Paulson, A.J. Fisher, D.M. DeLong, D.D. Parker and R.C. Nelson Helical liver CT with computer assisted bolus-tracking technology: Is it possible to predict which patients will not achieve a threshold of enhancement. *Radiology*,209, pages 787–792, 1998.

P. Rossi, A. Baert, W. Marchal, L. Tipaldi, W. Wilms and P. Pavone. Multiple bolus technique vs. single bolus or infusion of contrast medium to obtain prolonged contrast enhancement of the pancreas. *Radiology*,144(4), pages 929-931, 1982.

G.D. Schweiger , P.J. Chang and B.P. Brown Optimizing contrast enhancement during helical CT of the liver: a comparison of two bolus tracking techniques. *American Journal of Roentgenology*, 171(6), pages 1551–1558,1998.

G. Wang, G.M. Raymond, Y. Li, M. Sharafuddin, A. Stolpen,S. Yang, Z. Li, J.B. Bassingthwaighte and M. Vannier. A model on intervenous bolus propagation for optimization of contrast enhancement. *SPIE*,3978, pages 436–447, 2000.

Y. Wang, H.M. Lee, N.M. Khilnani, D.W. Trost, M.B. Jagust, P.A. Winchester, H.L. Bush, T.A. Sos and H.D. Sostman Bolus-chase MR digital subtraction angiography in the lower extremity. *Radiology*,207(1), pages 263–269, 1998.

Z. Wu and J. Qian. Real-time tracking of contrast bolus propagation in X-ray peripheral angiograph. *IEEE Workshop on Biomedical Image Analysis*, Santa Barbara, CA, 1998.

H. Yu, Y. Ye, S. Zhao and G. Wang. A backprojection-filtration algorithm for nonstandard spiral cone-beam CT with an n-PI-window. *Physics in Medicine and Biology*, 50(9), pages 2099-2111, 2005.